

THE REDUCTION OF NO WITH D₂ OVER THE (110) SURFACE OF IRIDIUM *

D.E. IBBOTSON **, T.S. WITTRIG *** and W.H. WEINBERG ****

Division of Chemistry and Chemical Engineering, California Institute of Technology, Pasadena, California 91125, USA

Received 17 February 1981; accepted for publication 21 July 1981

The heterogeneously catalyzed reaction between NO and D₂ to produce N₂, ND₃ and D₂O over Ir(110) was investigated under ultra-high vacuum conditions for partial pressures of the reactants between 5×10^{-8} and 1×10^{-6} Torr, total pressures between 10^{-7} and 10^{-6} Torr, and surface temperatures between 300 and 1000 K. Mass spectrometry, LEED, UPS, XPS and AES measurements were used to study this reacting system. In addition, the competitive coadsorption of NO and deuterium was investigated via thermal desorption mass spectrometry and contact potential difference measurements to gain further insight into the observed steady state rates of reaction. Depending on the ratio of partial pressures ($R \equiv P_{D_2}/P_{NO}$), the rate of reduction of NO to N₂ shows a pronounced enhancement when the surface is heated above a critical temperature. As the surface is cooled, the rate maintains a high value independent of temperature until a lower critical temperature is reached, where the rate drops precipitously. This hysteresis is due to a change in the structure and composition of the surface. For sufficiently large values of R and for an "activated" surface, N₂ and ND₃ are produced competitively between 470 and 630 K. Empirical models of the different regimes of the steady state reaction are presented with interpretations of these models.

1. Introduction

The reduction of NO by deuterium has been studied on the Ir(110)-(1 × 2) surface under ultra-high vacuum conditions with thermal desorption mass spectrometry, LEED, X-ray and UV-photoelectron spectroscopies, Auger electron spectroscopy and contact potential difference measurements. Both transient and steady state conditions were investigated. The motivation for this study is to elucidate the mechanism of a heterogeneously catalyzed reduction reaction, using the NO/D₂ system as a model.

* Supported by the National Science Foundation under Grant No. CHE77-16314.

** Present address: Bell Laboratories, 600 Mountain Avenue, Murray Hill, New Jersey 07974, USA.

*** Fannie and John Hertz Foundation Predoctoral Fellow.

**** Camille and Henry Dreyfus Foundation Teacher-Scholar.

Although much has been reported concerning the chemisorption of NO, hydrogen and CO on the transition metals, few studies have been carried out under low pressure, well characterized conditions for the heterogeneously catalyzed reduction of NO with either CO or hydrogen as the reducing agent. In ultra-high vacuum, the NO/H₂ system has been studied on polycrystalline Pt [1] and Pt(111) [2] under steady state conditions, and the NO/CO system has been studied on the (111) and (110) surfaces of Pt [3] and polycrystalline Rh [4] under transient conditions via thermal desorption mass spectrometry. At atmospheric pressure, the reduction of NO with CO or hydrogen under steady state conditions has been conducted over supported Pt, Pd, Rh and Ru [5,6].

Depending on the ratio of partial pressures of H₂ and NO ($R \equiv P_{\text{H}_2}/P_{\text{NO}}$) under steady state reaction conditions, the major products observed were H₂O, N₂ and NH₃ on polycrystalline Pt for surface temperatures between 300 and 900 K and a total pressure of approximately 10⁻⁷ Torr [1]. It was suggested that the limitation on the rate of the reduction reaction is related to the dissociation of NO [1]. For $R = 0.5$, the major products are N₂ and H₂O with N₂O formed as a minor product. However, for $R = 5$, NH₃, N₂ and H₂O are observed. In this case, NH₃ competes for nitrogen adatoms that are formed from the dissociation of NO. The reaction maximum at 495 K for the formation of NH₃ ($R = 5$) on polycrystalline Pt at low pressures [1] agrees well with the reaction maximum at 500 K observed on supported Pt at atmospheric pressure [5]. Good agreement is observed also for the temperature at which 50% reduction of NO occurs for similar values of R [1,5]. Thus, a connection has been established in this case between these widely different pressure regimes.

Steady state reaction experiments on Pt(111) [2] show that for excess NO, N₂ is the dominant product, and the rate of reduction is inhibited by NO below 550 K. In excess H₂, ammonia is the dominant product between 300 and 500 K, and above 500 K N₂ dominates. It was suggested from the steady state reaction data and from electron energy loss spectroscopic data that an ammonia-nitric oxide complex inhibits ammonia formation between 300 and 400 K on Pt(111) [2]. In agreement with the polycrystalline Pt results [1], on Pt(111) the formation of ammonia and nitrogen occurs competitively over a certain range of surface temperatures [2].

Investigations of the NO/H₂ system over various supported metals [5,6] reveal the selectivity of each catalyst with regard to the products formed. The overall reduction activity observed for NO/H₂ ($R = 4$) is Pd > Pt > Rh > Ru using the temperature at which 50% of the NO is reduced as the criterion. However, the major products formed are different among those metals. For Pd and Pt, NH₃ is formed preferentially; whereas for Rh and Ru, N₂ is the major product formed, more so for Ru [5]. The relationship between the product distribution in the reduction reaction and the facility of the metal to dissociate NO may well be the factor that determines the behavior of each metal. The ease of dissociation of NO occurs in the following order: Pd [7,8] < Pt [1-3,9,10] < Rh [4] < Ru [10-12]. The activity for NO dissociation on Ir [13-17] places this metal between Pt and Rh. Therefore,

it would be expected that the product distribution for the NO/H₂ system over Ir would be intermediate between Pt and Rh when the reduction reaction is performed under steady state conditions. This postulate will be tested for the present case of NO/H₂ over Ir(110).

The steady state reaction of NO and deuterium over Ir(110) has been examined for the partial pressure of the reactants varying from 5×10^{-8} to 1×10^{-6} Torr, the total pressure varying from 1×10^{-7} to 1×10^{-6} Torr, the surface temperature varying from 300 to 1000 K, and ratios of the partial pressures of the reactants, R , varying from 0.5 to 20. Both reactants and products were monitored with mass spectrometry during the steady state reaction. In order to assess the chemical composition of the overlayer under various conditions, XPS, UPS and AES measurements were performed. The degree of order in the overlayer–substrate system was monitored using LEED.

In addition, the nonreactive coadsorption of NO and deuterium at low temperature was investigated on Ir(110) as well as the rate of the transient reaction upon heating the surface on which these overlayers are present. Contact potential difference measurements of deuterium (NO) exposed to a surface partially covered with preadsorbed NO (deuterium) provide further insight into the competitive chemisorption of the two reactants. These data will supplement the previous studies of the chemisorption of NO [17] and deuterium [18] on Ir(110) and will aid in the interpretation of the steady state reduction reaction between NO and deuterium.

2. Experimental methods

The measurements were performed in an ion pumped stainless steel belljar that has been described previously [18,19]. The base pressure of reactive contaminants was below 2×10^{-10} Torr. A clean Ir(110) surface shows a (1×2) reconstruction, which is a surface with every other row of Ir atoms missing in the [001] direction according to a LEED intensity analysis [20]. This surface may be visualized as one containing alternate rows and troughs exposing (111) microfacets inclined to one another. Isotopic ¹⁵NO and D₂ [which has identical adsorption properties as H₂ on Ir(110)] were used in both the transient and steady state experiments to separate the mass spectrometric intensities for each of the products and reactants. Monitored species were D₂, D₂O, ¹⁵ND₃, ¹⁵N₂, ¹⁵NO, ¹⁵N₂O and ¹⁵NO₂. With the exception of the figure captions, the ¹⁵N species will be referred to without the superscript hereafter.

For both the transient and the steady state experiments, NO was exposed to the surface using a directional beam doser, where the pressure of the beam has been calibrated with the pressure of the storage bulb that supplies the dosing gas [17]. During the transient experiments involving coadsorbed overlayers of deuterium and NO, exposures of D₂ were performed via a leak valve. However, for the steady state reaction of D₂ and NO, both partial pressures of the reactant were exposed to the

surface via the directional beam doser with a known partial pressure of each gas admitted to the storage bulb of the doser. The calibration appropriate for the separate gases was the same as that when NO and D₂ were mixed in the bulb. Since the doser and the crystal were positioned so that part of the desorbing gases were in line-of-sight of the mass spectrometer, the intensities of the reactants and products could be measured directly (although this is not crucial to the results). Also, the gas flux from the doser does not load the ion pumps thus avoiding variations in the pumping speed since the beam-to-background pressure ratio for NO is approximately 100 : 1. Another advantage of the beam method is that wall effects caused by backfilling the reactor are minimized.

The steady state reaction sequence is as follows. For a given pressure ratio R and a total pressure P_T , the surface was annealed in vacuum above 1600 K to remove any contaminants. The surface was allowed to cool to near room temperature before it was exposed to the beam of reactants for 10 min to saturate the adsorbed overlayer fully. Then, the surface was heated ($<0.5 \text{ K s}^{-1}$), and the reactant and product intensities were measured every three seconds. Upon reaching the maximum temperature desired, the surface was cooled at approximately the same rate to near room temperature. In many temperature cycles, the temperature was held at various points for several minutes to ensure a steady state rate had been established. Under the chosen reaction conditions ($R \geq 0.5$), the intensity of D₂ did not vary measurably, and neither N₂O nor NO₂ were observed as reaction products.

3. Coadsorption of NO and deuterium

When NO is exposed to low precoverages of deuterium on Ir(110) at 100 K, the adsorption kinetics of NO are unchanged compared to adsorption of NO on a clean surface [17], as evidenced by the combined thermal desorption yields of NO and N₂. Fig. 1 presents thermal desorption mass spectra of NO, N₂, D₂O and D₂ from Ir(110). The surface was precovered first with 0.33 monolayer (ML) or $7 \times 10^{14} \text{ atoms cm}^{-2}$ of deuterium at 100 K, which saturates the most tightly bound state of deuterium [18], and subsequently various exposures of NO were applied. Heating the surface (20 K s^{-1}) produces various distributions of the desorption products, depending on the initial exposure of NO. Although the saturation coverage of NO ($9.6 \times 10^{14} \text{ cm}^{-2}$) is not affected by preadsorbed deuterium as evidenced by an N-atom mass balance in the thermal desorption spectra, the relative yields of NO and N₂ are different than those from the clean surface. Approximately 23% of the NO present initially desorbs as NO at saturation in fig. 1, whereas 35% desorbs as NO from the clean surface [17]. The fraction of NO desorbing from the high temperature feature is unchanged from the clean surface (18%) and represents desorption from a surface with oxygen present [17]. The fraction of NO desorbing from the low temperature feature is decreased (at saturation) from 17% to 5% when deuterium is preadsorbed. This feature represents desorption of NO from a surface

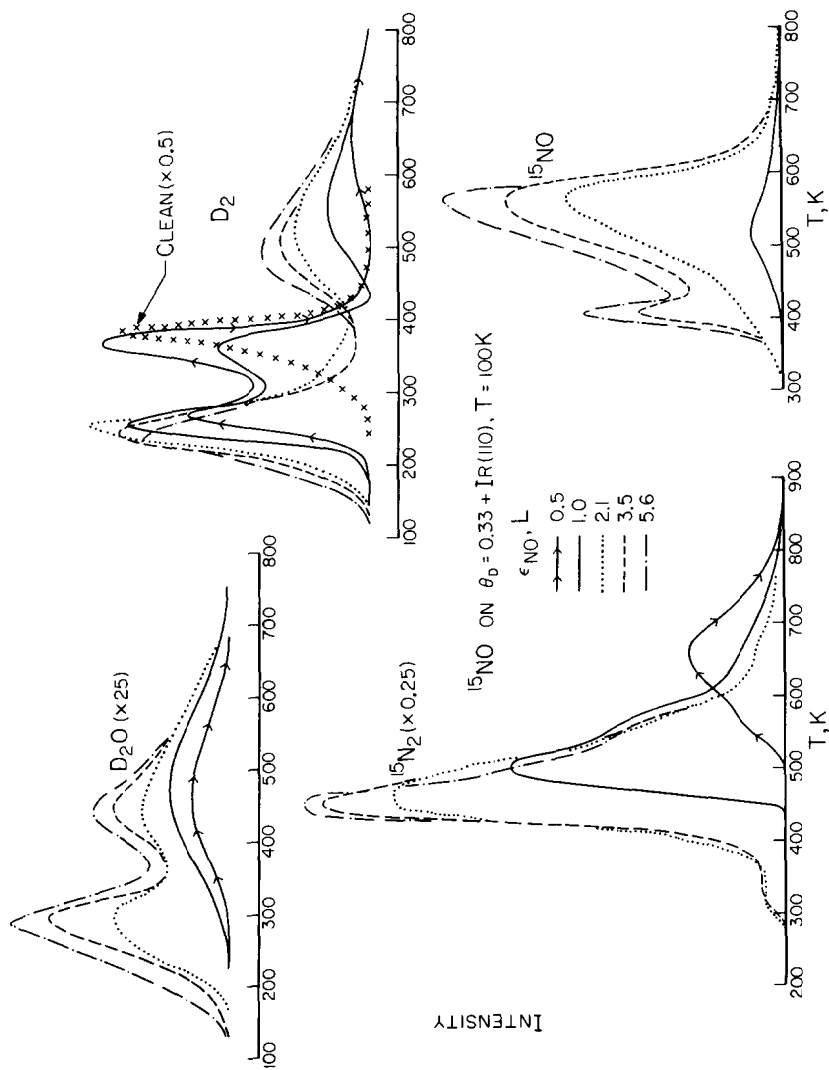


Fig. 1. Thermal desorption spectra from NO adsorbed on the β_2 -state of deuterium (0.33 ML) preadsorbed on Ir(110) at 100 K. The desorption products monitored are NO, N₂, D₂ and D₂O with a heating rate of 20 K s⁻¹. Under these conditions deuterium was not displaced from the surface as NO was adsorbed. For comparison, the desorption of the β_2 -state of deuterium is shown (x 0.5) in the absence of adsorbed NO.

free of oxygen. The temperature and shape of the desorption features of NO and N₂ are unchanged in fig. 1 compared to the clean surface. Therefore, low coverages of deuterium affect only the distribution of NO and N₂, i.e. the selectivity of the surface for nitrogen desorption.

The desorption of D₂ in fig. 1 is affected strongly by the presence of increasing coverages of NO as compared to the clean surface. Two peaks appear near 240 K and 490 K for the desorption of D₂ when the surface is saturated with NO compared to a single peak at 390 K when the surface is clean. The peak at 240 K is in the temperature region where D₂ desorbs from the low temperature state of deuterium when present at higher coverages on the clean surface [18]. Moreover, CPD measurements indicate that NO shifts deuterium from the high temperature state to the low temperature state as NO chemisorbs at 100 K. After the desorption maximum of D₂ at 240 K is passed, a desorption peak for D₂O occurs when the deuterium overlayer is saturated with NO as seen in fig. 1. Some dissociation of NO takes place below 300 K to cause D₂O to be formed, although the yield of D₂O is small ($\leq 5\%$ ML of oxygen reacted) since the curves are expanded by a factor of 25. Approximately 5% of the NO dissociates during adsorption near 300 K when deuterium is absent from the surface as seen by CPD measurements [17], and this is approximately the same fraction that dissociates as the surface is heated in this case inferred by the maximum yield of the low temperature D₂O desorption. The higher temperature peaks of D₂ (490 K) and D₂O (440 K) are of low intensity but are quite broad. These occur in the same temperature range where N₂ and NO desorb. In this region, the surface has large coverages of oxygen and NO and low coverages of deuterium and nitrogen adatoms. As the temperature increases, the concentration of deuterium adatoms decreases causing the formation of D₂ to dominate over D₂O both due to the greater mobility of deuterium compared to oxygen and the fact that diatomic recombination (D₂) is more likely than triatomic recombination (D₂O).

Thermal desorption mass spectra of reaction products from a surface prepared with a saturated overlayer of NO under three different conditions and then exposed to 2 L D₂ are presented in fig. 2. As in fig. 1, the yield of D₂O is low compared to D₂, but in fig. 2 the yield of D₂ is lower than in fig. 1. The desorption of D₂ at high temperature occurs as NO and N₂ desorb in fig. 2, as in fig. 1. Again, the temperature at which N₂ and NO desorb is not affected by exposures of D₂ if the overlayer of NO is saturated at 100 K. Also the distribution of N₂ and NO is the same as if no deuterium were adsorbed. However, the desorption results for the other two surface preparations are not so obvious. The concentration of deuterium that chemisorbs does not depend in a simple way upon the coverage of NO and the coverage of oxygen. Adsorbing NO at 450 K, cooling and exposing it to 2 L D₂ at 100 K causes the surface composition to be 0.51, 0.31 and 0.20 fractional coverages of oxygen, NO and deuterium, respectively. Saturating the surface at 100 K with NO and then exposing to 2 L D₂ allows 0.33 fractional coverage of deuterium to chemisorb. Annealing the saturated overlayer of NO at 100 K to 400 K, cooling to 100 K and

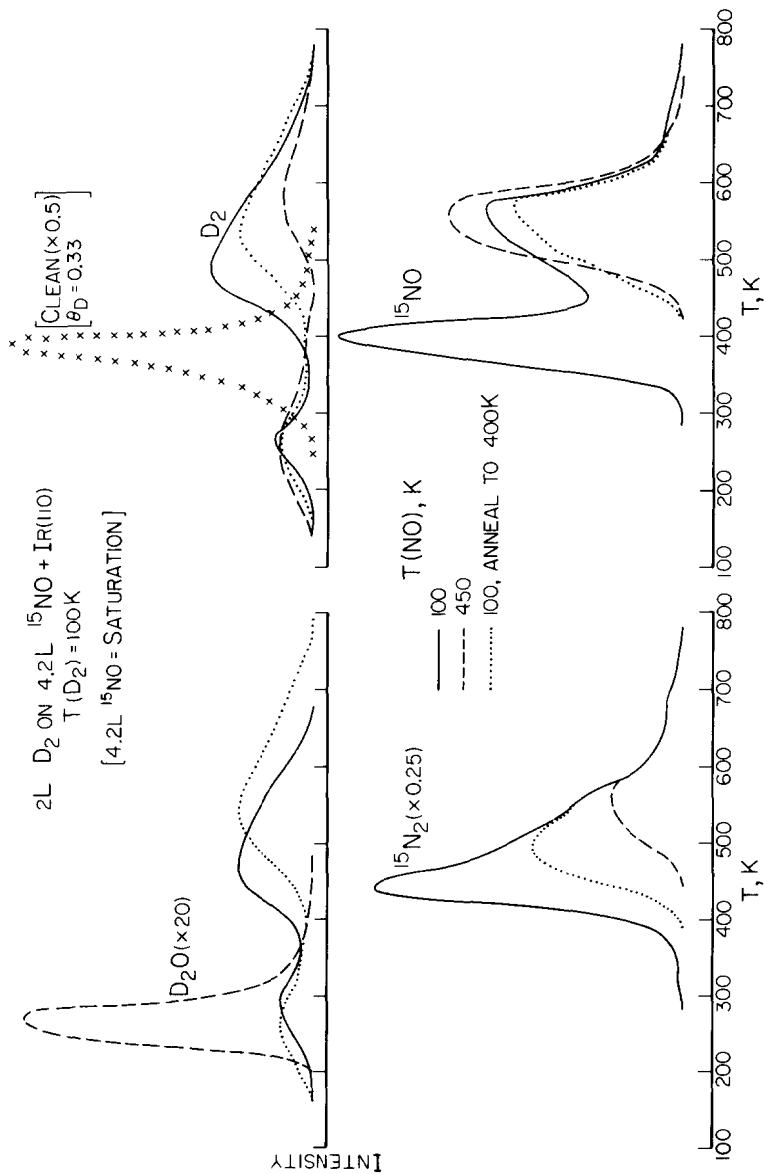


Fig. 2. Thermal desorption spectra of NO, N₂, D₂ and D₂O from 2 L D₂ adsorbed on various surfaces of Ir(110) at 100 K prepared with saturation exposures of NO: (—) saturated overlayer of NO adsorbed at 100 K; (- - -) saturated overlayer of NO adsorbed at 450 K and cooled to 100 K; (· · · · ·) saturated overlayer of NO adsorbed at 100 K and annealed briefly to 400 K. The heating rate is 20 K s⁻¹.

exposing to 2 L D₂ causes the surface composition to be 0.32, 0.51 and 0.23 fractional coverages of oxygen, NO and deuterium. Also, 2 L D₂ exposed to a saturated oxygen overlayer results in the adsorption of approximately 0.3 ML of deuterium. Saturating the surface with oxygen and then saturating further with NO (<0.5 ML) blocks deuterium adsorption completely. This observation will be pertinent to the steady state reaction of NO and D₂ presented in the following section. Finally in fig. 2, the desorption temperature for D₂O and the yields of N₂ and NO depend on the relative initial surface coverages of NO and oxygen. Adsorbing NO at 450 K and adsorbing deuterium at low temperature allows deuterium to react with oxygen to form D₂O more readily than the other two surface preparations in fig. 2. Comparing the NO/N₂ desorption yields in this case and for the surface prepared by annealing a saturated overlayer of NO to 400 K shows that the presence of oxygen tends to cause increasing amounts of NO to desorb rather than N₂, as observed when no deuterium is present [17].

In order to gain additional insight into the competitive adsorption of NO and deuterium (hydrogen), CPD measurements of NO (D₂) on deuterium (NO) overlayers were performed on Ir(110) at 100 K. The CPD of NO is presented in fig. 3 as a function of fractional coverage for NO adsorbed on (a) a clean surface [17], and (b) a surface with 0.33 ML deuterium adsorbed initially (β_2 -state [18]). Note that the CPD of NO in fig. 3a decreases weakly with coverage, attains a minimum near 0.5 ML and increases slightly near 0.8 ML as the completion of a disordered superstructure is reached [17]. However, the CPD of NO in fig. 3b exposed to the β_2 -state of deuterium shows a much larger decrease and a different shape than fig. 3a. As seen in fig. 1, the β_2 -state of deuterium is displaced by NO into the β_1 -state.

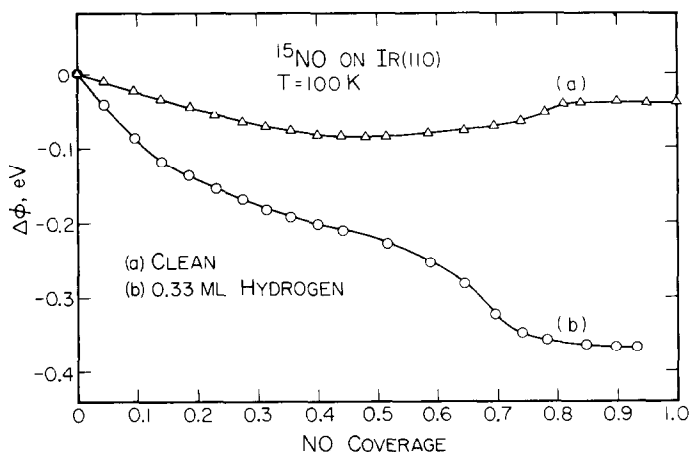


Fig. 3. The CPD of NO adsorbed at 100 K on Ir(110) as a function of the fractional coverage of NO. (a) Clean surface; and (b) preadsorbed β_2 -state of deuterium (or hydrogen) (0.33 ML).

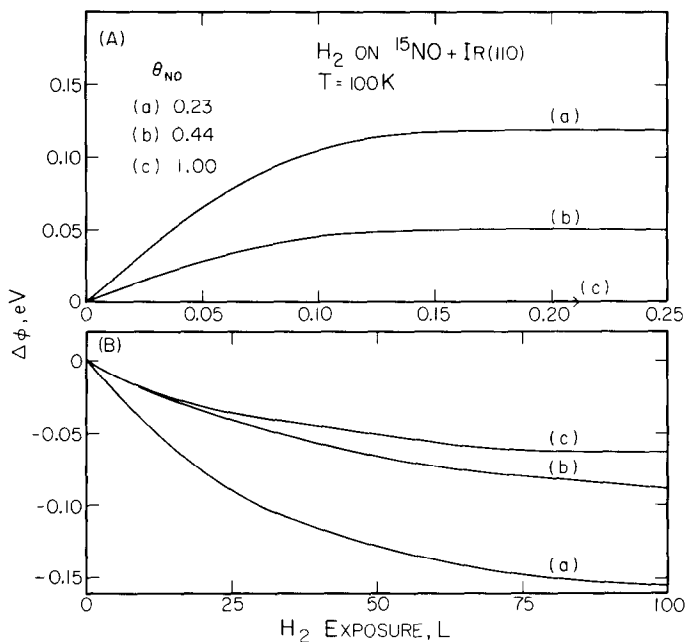


Fig. 4. The CPD of H₂ (or D₂) adsorbed on fractional coverages of NO on Ir(110) at 100 K: (a) 0.23; (b) 0.44; (c) 1.00. In (A) the exposure of H₂ is sufficient to saturate the β_2 -state, and in (B) the exposure of H₂ includes part of the β_1 -state (see text). The zero in (B) for the CPD is equal to the "saturation" value (at 0.25 L H₂) in (A).

Also, for the chemisorption of deuterium on Ir(110) [18], the CPD of deuterium increases by 0.30 eV for the β_2 -state and decreases weakly with coverage as the β_1 -state is populated. Therefore, the change in the CPD behavior of NO in fig. 3b (β_2 -state adsorbed) from fig. 3a (clean) is due to the displacement of deuterium in the β_2 -state to the less tightly bound β_1 -state, verifying the thermal desorption results in fig. 1.

The CPD of deuterium (or hydrogen) monitored as a function of exposure to a surface with different precoverages of NO provides complementary data to that of fig. 3, and these results are shown in fig. 4. In fig. 4A, the CPD of deuterium is presented over the exposure range required to saturate the β_2 -state, and in fig. 4B the CPD of deuterium is shown over that part of the exposure range pertinent to the β_1 -state. Recalling that for the β_2 -state of deuterium the CPD increases by 0.30 eV on the clean surface, it is clear that the β_2 -adsorption sites are blocked significantly as the coverage of NO increases. For a saturation coverage of NO, the CPD of deuterium does not change (curve (c)) indicating that the β_2 -sites of deuterium are blocked completely. Since the adsorption kinetics of deuterium were not measured as a function of the precoverage of NO, the relationship between the

coverage of NO and the coverage of deuterium cannot be quantified further. Over the exposure range of the β_1 -state of deuterium in fig. 4B, NO blocks these adsites as well.

In summary, the coadsorption of deuterium and NO has been studied with thermal desorption mass spectrometry and CPD measurements to gain insight into the kinetics of adsorption and desorption compared to the kinetics of adsorption and desorption in the case of the adsorption of NO and deuterium separately. Saturating a surface that is precovered with the β_2 -state of deuterium (0.33 ML) with NO gives the same saturation coverage of NO, but upon desorption more N₂ desorbs (from the dissociation of NO) than from a surface with no deuterium present. The desorption shapes and peak temperatures of NO and N₂ are not perturbed by the presence of deuterium, but the desorption of D₂ is changed significantly compared to the clean surface. Saturating the surface with NO does not block the subsequent adsorption of deuterium completely. However, an overlayer saturated with NO and oxygen, a condition that occurs during the steady state reaction at low temperatures (see the following section), blocks the chemisorption of deuterium completely. On a surface free of oxygen, NO displaces deuterium from its preferred sites (β_2) in the missing row troughs into the less tightly bound sites (β_1) along the (111) microfacets exposed on the Ir(110)-(1 × 2) surface [18].

4. Steady state reaction between NO and deuterium

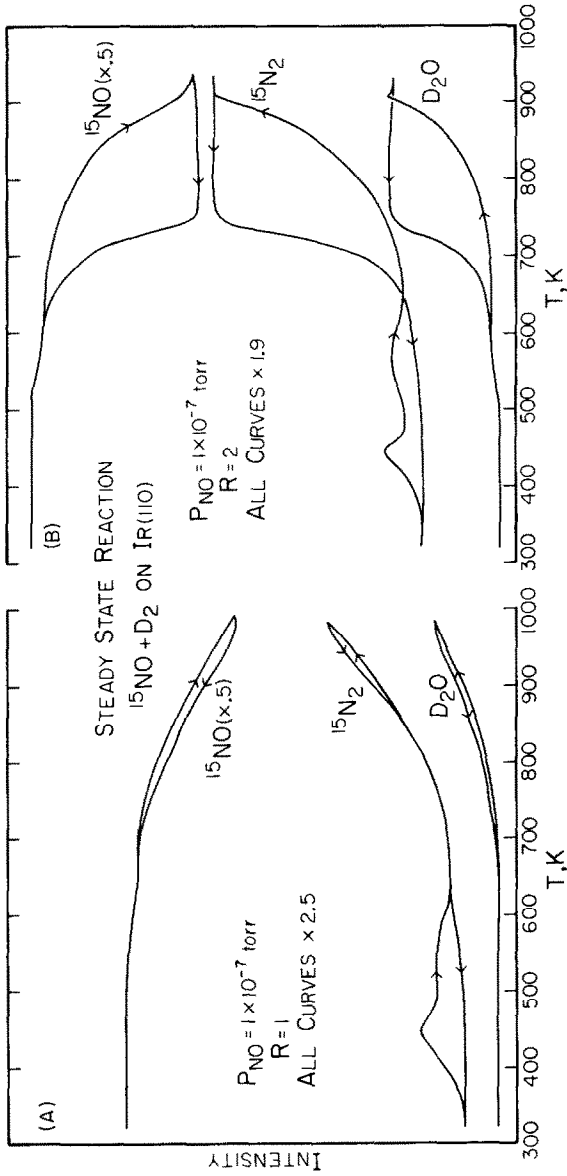
The reduction of NO with deuterium over Ir(110), as measured by mass spectrometry under steady state conditions, is presented in this section. The procedure used to carry out the steady state experiments was described in section 2. Under all conditions examined, i.e. partial pressure ratios (R) between 0.5 and 20, temperatures between 300 and 1000 K and total pressures between 5×10^{-8} and 1×10^{-6} Torr, the partial pressure of D₂ did not vary significantly (<10%), and neither N₂O nor NO₂ was observed. Typically, the total time required to measure a reaction cycle was between 30 and 60 min, where a cycle refers to heating to the maximum temperature desired and cooling to near room temperature. During a reaction cycle, the pressure in the storage bulb that supplies the reaction mixture to the Ir(110) catalyst decreased by less than 5% in any particular experiment, and this decrease could be accounted for, as necessary, since the decrease is approximately linear with respect to time. Finally, the gain of mass spectrometer that was used to monitor the reactants and products during the steady state reaction was measured after each set of reaction cycles in order to compare relative reaction rates between several sets of data.

Reaction cycles corresponding to a set of four ratios of partial pressures ($R = 1, 2, 4$ and 8) at $P_{\text{NO}} = 1 \times 10^{-7}$ Torr are shown in figs. 5A–5D, presenting the mass spectrometric intensities (shifted for clarity) of NO, N₂, D₂O and ND₃ (fig. 5D only) as a function of surface temperature. The direction of the arrows on

each curve indicates whether the surface temperature is increasing or decreasing. The initial rise in N₂ production near 440 K is seen always in the first reaction cycle for all reaction conditions presented here, but never in succeeding reaction cycles *if the surface is not cleaned of oxygen*. This rise in N₂ production is not followed by a decrease in the NO intensity or by an increase in the D₂O intensity as required by mass balance. The N₂ peak is due to the surface initially containing a large coverage of NO near room temperature converting to a surface containing a large coverage of oxygen and NO. Thus, the surface conversion causes an *apparent* increase in the steady state rate of production of N₂. However, this initial desorption of N₂ is a *nonsteady state conversion* which depends only upon the rate at which the surface is heated. A second maximum in the rate of production of N₂ that occurs near 540 K is seen in most reaction cycles, and this is followed by a decrease in the intensity of NO and an increase in the intensity of D₂O. Consequently, this is due primarily to a steady state surface reaction although part of this peak may be due to the surface conversion of some chemisorbed oxygen to a surface oxide which begins to form near this temperature [21], or it may be associated with a peak seen in thermal desorption spectra of NO and N₂ [17].

As the surface temperature increases in fig. 5A, the N₂ and D₂O production increases with a concomitant decrease in the measured intensity of NO. The temperature was decreased after attaining a maximum value of 980 K, and a slight hysteresis occurred, i.e. a different rate of reaction is measured at the same temperature compared to when the surface is heated. Below 600 K, the rate production of N₂ did not follow the upward reaction curve for the reason stated earlier concerning the "clean surface" conversion to one which contains a surface oxide as well as chemisorbed oxygen. Succeeding cycles for surfaces not cleaned by annealing to 1600 K follow closely the curve for decreasing temperature in the first cycle.

In contrast to the results for R equal to one in fig. 5A, the reaction for R equal to two and four in figs. 5B and 5C is quite different at high temperatures. As the temperature increases, a plateau is reached in the production of N₂ that, once reached, persists at lower temperatures. An abrupt increase in the production of D₂O occurs at the onset of the N₂ plateau and thereafter maintains a constant value as well. As the temperature decreases further, the rate of the production of N₂ (NO reduction) decreases and eventually reaches the value observed as the temperature of the surface was increased. Both the onset and the drop-off of the N₂ plateau depend upon the value of R as seen in figs. 5B and 5C. As P_{D_2} increases, the temperature of the onset and the drop-off in the N₂ plateau both decrease. Moreover, the magnitude of the rate increases with P_{D_2} , noting that the reaction curves have been expanded differently. Although a constant rate of production of D₂O is seen in fig. 5D as the temperature is decreased, the rate of production of N₂ does not remain constant. The decrease in the production of N₂ is due to the production of ND₃ that competes for nitrogen adatoms. The rate of production of ND₃ reaches a maximum near 560 K.



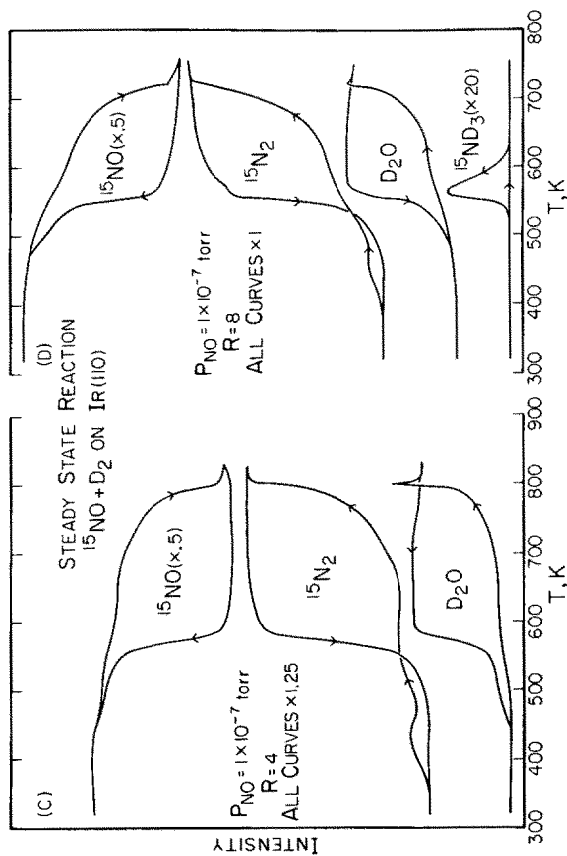


Fig. 5. Steady state reaction for NO + D₂ over Ir(110). $P_{\text{NO}} = 1 \times 10^{-7}$ Torr, and $R (= P_{\text{D}_2}/P_{\text{NO}})$ equal to: (A) 1; (B) 2; (C) 4; (D) 8. The intensities monitored in the gas phase are NO, N₂, ND₃, D₂ and D₂O. For all values of R , the intensity of D₂ did not vary appreciably in a reaction cycle, and it is not shown here or in following figures. Arrows pointing to the right (left) indicate the surface temperature is increasing (decreasing). Ammonia (ND₃) production occurs in (D) only.

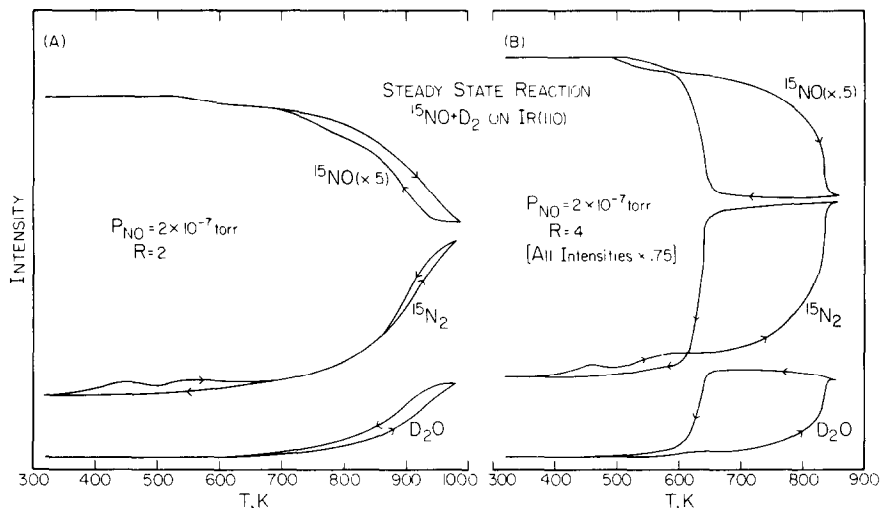


Fig. 6. Steady state reaction for NO + D₂ over Ir(110). $P_{\text{NO}} = 2 \times 10^{-7}$ Torr, and R equal to: (A) 2; (B) 4. No ND₃ is produced under these conditions.

Doubling the partial pressure of NO (P_{NO}) for R equal to two inhibits the formation of a plateau in the rate of production of N₂ as seen in fig. 6A. These curves are similar to those in fig. 5A in that both do not contain a plateau, but some hysteresis occurs at high temperature. Thus, the existence of a plateau (high reduction rate) does not depend on R only but depends also on the absolute value of P_{NO} . Doubling P_{D_2} (compare figs. 6B and 6A) causes the N₂ plateau to appear near 840 K, and the curves are similar to those of figs. 5B and 5C.

The last set of reaction curves is presented in fig. 7 where the production of ND₃ is maximized by the use of a low pressure of NO and large values of R . For $P_{\text{NO}} = 5 \times 10^{-8}$ Torr and $R = 8$ (fig. 7A), the plateau in the rate of production of N₂ occurs near 700 K, accompanied by an abrupt increase in the rate of production of D₂O, as seen previously. As the temperature decreases, the intensity of N₂ varies more strongly than was observed in fig. 5D where ND₃ was first detected. In fact, a relative minimum and a relative maximum occur in the N₂ curve which are directly associated with the maximum rate of production of ND₃ appearing near 540 K. Once the relative maximum in the production of N₂ is passed at 520 K, the rate of reaction falls precipitously, and the shape of the dropoff depends upon the rate of the temperature decrease, i.e. the rate decreases in a smaller temperature range than shown here.

The final reaction cycle, presented in fig. 7B, represents the most favorable conditions to produce ND₃ examined on Ir(110), namely, $P_{\text{NO}} = 5 \times 10^{-8}$ Torr and $R = 20$. In fig. 7B, the onset of a high rate of reaction does not occur abruptly, as seen previously. Moreover, a small rate of production of ND₃ occurs as the temperature

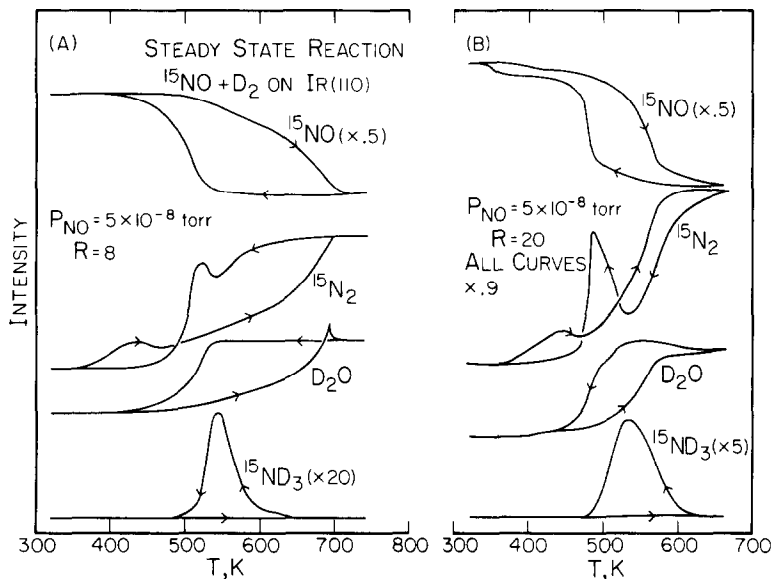


Fig. 7. Steady state reaction for NO + D₂ over Ir(110) under conditions that favor the production of ND₃. $P_{\text{NO}} = 5 \times 10^{-8}$ Torr, and R equal to: (A) 8; (B) 20.

increases. As the surface temperature decreases, the competition between the production of N₂ and ND₃ favors the formation of ND₃ which reaches a maximum near 530 K. This can be seen by a mass balance of ND₃ and N₂ with respect to NO. Again, the rate of production of N₂ attains a relative maximum as the production of ND₃ falls to zero.

In summary, figs. 5–7 provide representative data that may be used to understand the competing processes which are important during the steady state reduction of NO with D₂ (or H₂). It is apparent that the formation of N₂ and ND₃ compete for nitrogen adatoms, provided by the decomposition of NO, when a large excess of D₂ is present in the reaction mixture. Other factors depend strongly on the values of R as well, such as whether or not a plateau in the production of N₂ is formed, the magnitude of the rate of reduction, and the temperature range over which the N₂ plateau is stable. Three reaction regimes are of interest: (1) the reduction reaction prior to the “activation” of the surface region regardless of whether or not a plateau exists in the reaction cycle, (2) the plateau in N₂ production, and (3) ND₃ production. Each of these reaction regimes will be examined with respect to the structure of the overlayer and substrate, composition of the adlayer, and the pressure dependence of the reactants on the rate of reduction.

Three production cycles of N₂ are shown in fig. 8 that were presented in the previous figures but are expanded here to show clearly the changes caused by varying the partial pressures of the reactants. Increasing P_{NO} at a constant P_{D_2}

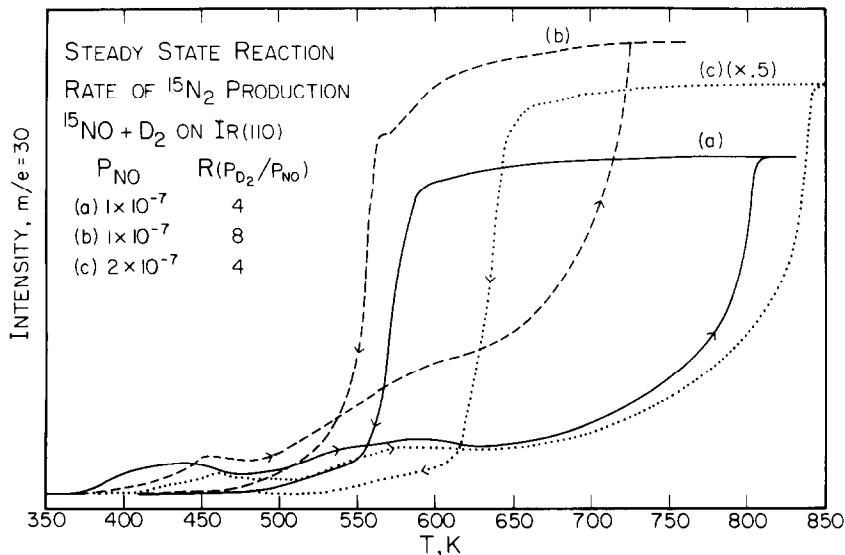


Fig. 8. Steady state rates of N₂ production from figs. 5 and 6. (a) $P_{NO} = 1 \times 10^{-7}$ Torr and $R = 4$; (b) $P_{NO} = 1 \times 10^{-7}$ Torr and $R = 8$; (c) $P_{NO} = 2 \times 10^{-7}$ Torr and $R = 4$. The intensity of N₂ has been expanded by 0.5 in (c). Note that in (b) some ND₃ is produced near the drop-off in N₂ production, as the temperature is decreased.

(figs. 8b and 8c) increases the temperature for the onset and dropoff of the N₂ plateau, increases the rate of production of N₂ on the plateau, and decreases the rate of production of N₂ before the plateau is reached. The latter two observations are for a constant temperature which allows the same reaction regime to be compared. Maintaining P_{NO} constant and increasing P_{D_2} (figs. 8a and 8b) decreases the temperature for the onset and drop-off of the N₂ plateau and increases the rate of production of N₂ both on the plateau and before the plateau.

In order to clarify the reduction reaction when N₂ is the primary nitrogen-containing product, the dependence of the rate below and on the N₂ plateau was fit empirically as a power law of the partial pressures of the reactants. For the rate of production of N₂ at low rates (T increasing), either in the presence or the absence of a plateau, the rate may be expressed as

$$R_{N_2} = cP_{NO}^{-1/2}P_{D_2}, \quad (1)$$

at a constant temperature. Also, on the N₂ plateau at temperatures where N₂ only is produced, the rate of production of N₂ is described by

$$R_{N_2} = c'P_{NO}P_{D_2}^{1/2}. \quad (2)$$

For a given set of partial pressures of D₂ and NO, the rate of reaction of N₂

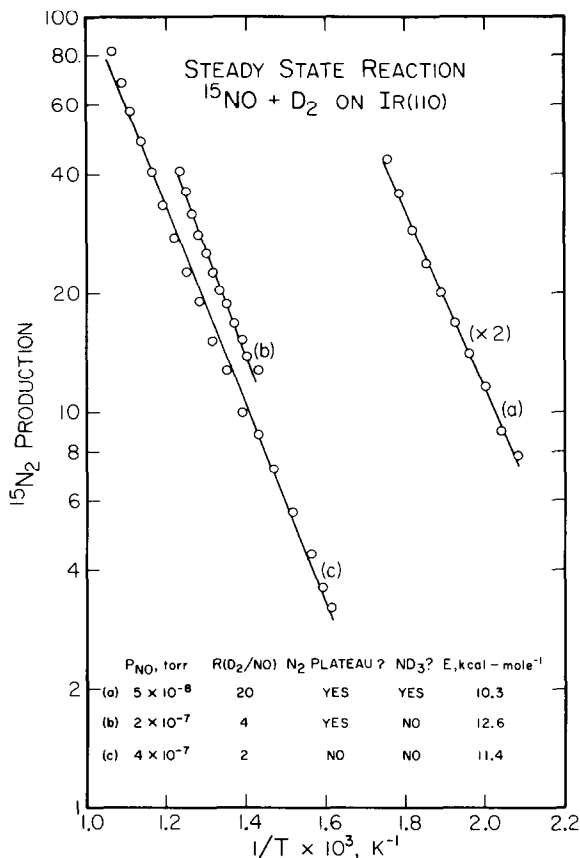


Fig. 9. The temperature dependence of the rate of production of N₂ as the temperature increases but before a plateau is reached (if it is present). Three different reaction conditions are presented, as noted in the figure, for ln R_{N₂} as a function of T⁻¹. The slope of each curve is proportional to the effective activation energy for the reaction, which is presented as well.

below the plateau) as the surface temperature increases may be written as

$$R_{N_2} = \Gamma P_{D_2} P_{NO}^{-1/2} \exp(-E/kT), \quad (3)$$

using the empirical expression in eq. (1), and writing out the term c in eq. (1) as $\Gamma \exp(-E/kT)$. Plotting $\ln R_{N_2}$ as a function of T^{-1} should give a straight line if this expression is appropriate, and three of these experimental plots are shown in fig. 9 over the range of conditions observed. All three cases: (1) no N₂ plateau, (2) a N₂ plateau, and (3) a N₂ plateau with production of ND₃, are included in fig. 9. The slope of each straight line in fig. 9 gives the effective activation energy, E , for the reaction. In fig. 9, E varies from 10.3 to 12.6 kcal mole⁻¹, and all other slopes that

were calculated lie in this range. The intercepts of the lines in fig. 9 are proportional to $\Gamma P_{D_2} P_{NO}^{-1/2}$. Once a calibration is obtained for R_{N_2} , the value of Γ may be calculated, and it was found to be equal to $1 \times 10^{19 \pm 1}$ molecules $\text{cm}^{-2} \text{s}^{-1} \text{Torr}^{-1/2}$. The error limits are estimates of the bounds due to the averaging of each experimental curve plotted.

Turning to the pressure dependence of the production of ND₃ at the ND₃ reaction maximum, the rate fits the following relation

$$R_{ND_3} = c'' P_{D_2}^2 P_{NO}^{-1}, \quad (4)$$

including all experimental conditions that produce ND₃. The interpretation of this expression, as well as the other empirical rate expressions, will be discussed in section 6. Several experimental conditions that produce ND₃ in appreciable quantities are shown in fig. 10. The rate of production of ND₃ is shown only as a function of surface temperature for $P_{NO} = 5 \times 10^{-8}$ Torr and R varying from 4 to 20. From fig. 10, the rate of production of ND₃ does not vary with respect to the tempera-

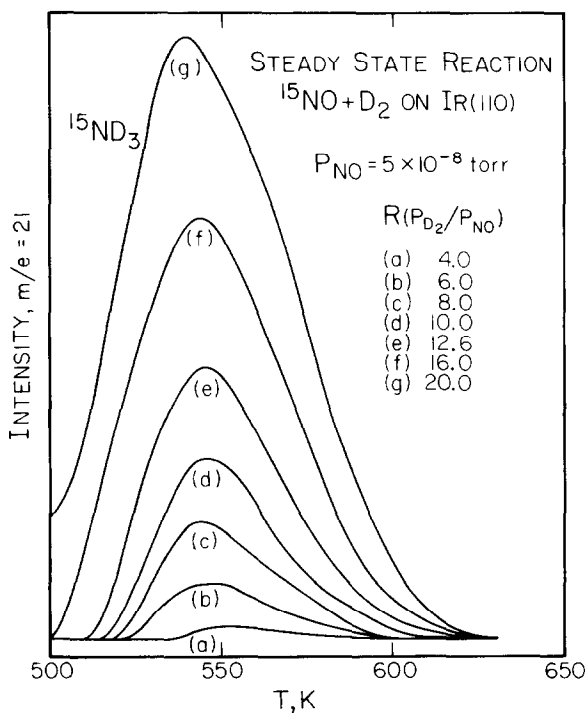


Fig. 10. Steady state rate of ND₃ production for $P_{NO} = 5 \times 10^{-8}$ Torr and R equal to: (a) 4.0; (b) 6.0; (c) 8.0; (d) 10.0; (e) 12.6; (f) 16.0; (g) 20.0.

ture at which the maximum rate occurs (545 K), and it exhibits asymmetric behavior with a high temperature tail that broadens as R increases.

In summary, experimental reduction reaction cycles have been presented to show the widely different rates in the reduction of NO that occur on Ir(110) as the surface temperature and the partial pressures of the reactants vary. Also, the reduction products containing nitrogen (N₂ and ND₃) are formed in different distributions that depend upon the partial pressures of the reactants. The dependence of the reaction rate of N₂ and ND₃ on the partial pressures of the reactants has been derived empirically from the experimental curves. The results of this section will be combined with the results that will be presented in the following section, and they will be discussed together in section 6.

5. XPS, UPS, AES and LEED results

Several XPS and UPS measurements were performed to determine the chemical composition of the adlayer at various points during the steady state reaction. Also, LEED was used to monitor the order in the adlayer at similar points in the steady state reaction.

During the steady state reaction under various conditions, the reaction was terminated by suddenly cooling ($>50 \text{ K s}^{-1}$ in the reaction region) the Ir(110) surface and rotating it away from the reactant flow in the dosing beam. The surface was then analyzed in the N(1s) and O(1s) regions of binding energy by XPS and in the valence band region by He I UPS. Identical spectra may be obtained by cooling to below room temperature. In fig. 11 (XPS) and in fig. 12 (UPS), three points in the steady state reaction are shown for $P_{\text{NO}} = 5 \times 10^{-8}$ Torr: (a) $R = 10$, quenched at the ND₃ reaction maximum (540 K); (b) $R = 10$, completion of a reaction cycle; and (c) $R = 1$, completion of a reaction cycle. When the reaction is terminated at the ND₃ reaction maximum, the N(1s) region in fig. 11 shows one feature centered at 396.7 eV due to nitrogen adatoms. Under the same conditions, the O(1s) region shows one low-intensity feature centered near 530.5 eV. The corresponding result with UPS (fig. 12a) yields an emission of low intensity between 5 and 6 eV below the Fermi level, E_{F} , due mainly to the nitrogen 2p orbital. The emission in the O(1s) region of binding energy at 530.5 eV may be caused by hydroxyl groups which exhibit this binding energy on Ir(110) [22]. However, no corresponding UPS features are observed which would be expected near 11.1 and 7.8 eV as on Pt(111) [23]. Thus, the assignment of the O(1s) peak in fig. 11a is subject to question, but it is of rather low intensity.

Performing the steady state reaction for $R = 10$ through a complete cycle and then recording the XP and UP spectra yield the results shown in figs. 11b and 12b. The N(1s) binding energy region has a single peak at 400.1 eV with a large high binding energy tail both of which are due to adsorbed NO [17]. The O(1s) region has a peak due to adsorbed NO at a binding energy of 531.5 eV, and oxygen

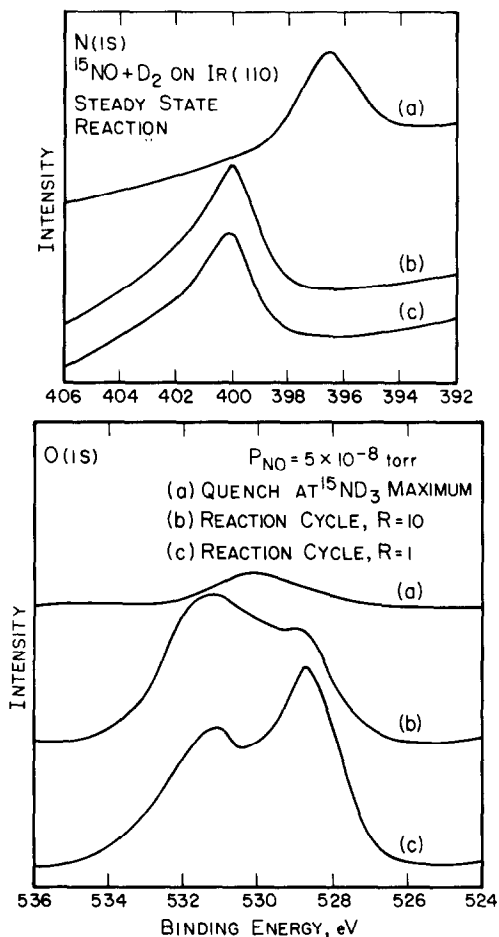


Fig. 11. XPS ($h\nu = 1486.6$ eV) for the N(1s) and the O(1s) regions of binding energy, relative to the Fermi level, at three points in the steady state reaction. $P_{\text{NO}} = 5 \times 10^{-8}$ and (a) $R = 10$ at the ND_3 reaction maximum; (b) $R = 10$ after a reaction cycle; and (c) $R = 1$ after a reaction cycle. For each spectrum, the reaction was terminated by simultaneously removing the Ir(110) surface from the reactant gas beam and cooling to near room temperature.

adatoms are present as well as evidenced by the peak near 528.8 eV. Adsorbed NO is indicated in the UP spectra of fig. 12b as judged by emission at 8.5 and 10.4 eV due to the 1π and 5σ orbitals of molecular NO [17]. The emission near 12.8 eV is due to the 4σ orbital but has shifted from its value on the clean surface at low temperature, 13.5 eV. Similar to fig. 12a, emission is seen also near 6 eV in fig. 12b which, in this instance, is due to the oxygen 2p orbital.

The reaction cycle for $R = 1$, represented in figs. 11c and 12c by the XPS and

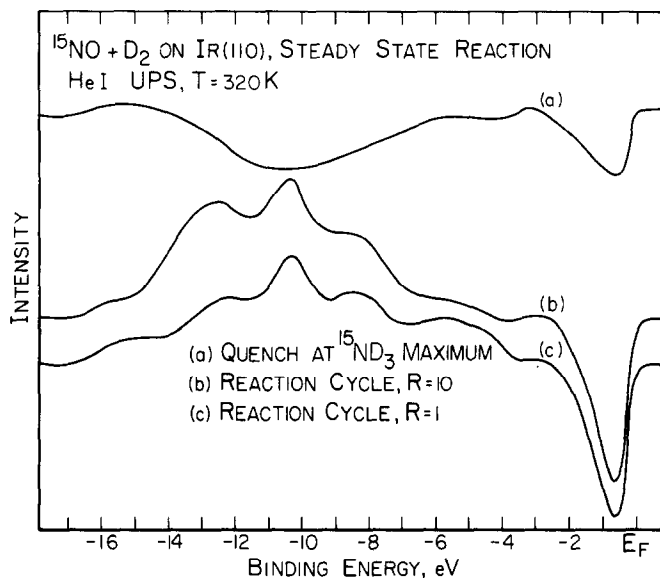


Fig. 12. He I UPS ($h\nu = 21.2$ eV) of Ir(110) near room temperature for three points in the steady state reaction. The corresponding conditions for (a)–(c) are given in fig. 11.

UPS measurements, indicates only one nitrogen-containing species, NO, is present here as for the case of $R = 10$. However, the concentration of NO is smaller and the concentration of chemisorbed oxygen is larger, as seen in figs. 11c compared to figs. 11b. In agreement with this, the valence orbitals in fig. 12c are of lower intensity for adsorbed NO, and the O 2p emission near 6 eV is larger. The orbitals of NO are not perturbed greatly in the reaction cycles compared to the clean surface [17].

The Auger KLL transitions of nitrogen adatoms were measured after terminating the reaction at the ND₃ rate maximum. Two features are seen in fig. 13 at kinetic energies of 385.7 and 372.5 eV for the N-KLL region. Two features were observed also for nitrogen adatoms on polycrystalline Pd [24] at similar kinetic energies. The transition at 385.7 eV involves the N 2p levels, and the transition at 372.5 eV involves both the 2p and 2s orbitals of the nitrogen adatoms, as calculated from a simple approximation for the Auger transitions [25].

Finally, LEED observations were made after the reaction was terminated. For low values of R which do not cause a plateau in production of N₂, an imperfect oxygen c(2 × 2) overlayer structure is observed as the rate of production of N₂ increases with surface temperature, and this represents oxygen chemisorbed on the *unreconstructed* (1 × 1) surface that is stabilized by a surface oxide [21]. The degree of order of this LEED superstructure depends upon the reaction conditions. After termination of the reaction, if the temperature were lower or if R were larger,

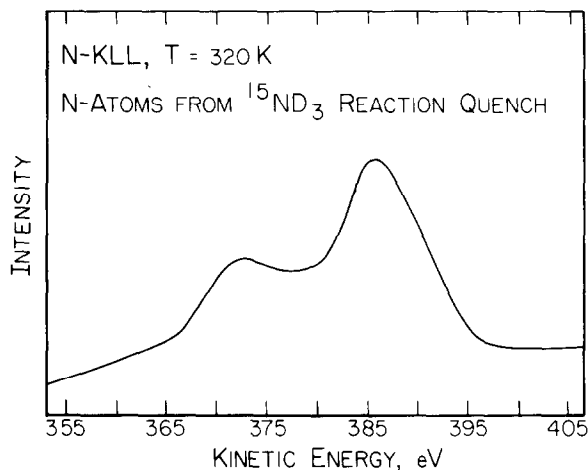


Fig. 13. Auger electron spectrum of the N-KLL region of energy. The steady state reaction was terminated for this spectrum at the ND₃ reaction maximum proceeding under the same conditions as in figs. 11a and 12a.

the order in the overlayer was always (qualitatively) less. After the reaction cycle was completed for low values of R and the surface cooled to near room temperature, a (1×2) LEED superstructure was observed with sharp integral order spots and large, diffuse half-order spots. This superstructure does not correspond to the reconstructed (1×2) substrate since the half-order substrate spots are not large and diffuse but rather are streaked in the $[001]$ direction if the substrate is somewhat disordered. Rather, this overlayer is due to approximately 0.5 ± 0.05 ML of both NO and oxygen. This superstructure was observed also if an oxygen $c(2 \times 2)$ superstructure was formed, and then the overlayer was saturated with NO at 300 K [17]. Thus, the (1×2) pattern is a superstructure of NO and oxygen coadsorbed on the Ir(110)- (1×1) surface.

If the value of R is sufficiently large to achieve a plateau in the rate of production of N₂, the LEED superstructure is a sharp (1×2) which is a clean and reconstructed substrate pattern. The coverages of NO and oxygen are less than 2% as measured by thermal desorption mass spectrometry. As the surface temperature decreases (with sufficiently large R) and the maximum rate in production of ND₃ is reached, the LEED pattern shows streaks between the substrate spots in the $[001]$ direction with some modulation of intensity (after the reaction is terminated and the surface is cooled to room temperature). From the XPS, UPS and AES results, only nitrogen adatoms are present, and this pattern is probably a poorly ordered $p(2 \times 2)$ superstructure on Ir(110)- (1×2) . Near the drop-off in the production of N₂ at low temperature, LEED shows a (1×2) superstructure with streaking along and between the substrate spots and a higher background than before the drop-off. The streaking along the substrate spots is reminiscent of chemisorbed oxygen [21],

and the streaking between the rows is due to both oxygen and nitrogen adatoms. Once the reaction cycle is complete (for $R > 4$), the (1 × 2) substrate is still observed at room temperature, but the background is quite high, as it appears when the surface is saturated with NO at 300 K or below [17].

In the following section, the results of this section and section 4 will be discussed in order to understand the various steps in the reaction between NO and D₂ over Ir(110). Modelling of the elementary steps will be limited to building qualitatively a conceptual model due to the rather complex competing processes which occur as the reaction proceeds.

6. Discussion

As seen from the data presented in the previous sections, the reduction of NO with hydrogen over Ir(110) is quite complex. Depending on the surface temperature and the partial pressures of the reactants, the rate of reduction and the product distribution vary considerably. Moreover, the nature of the catalytic surface (whether the surface is clean or oxidized) during a reaction cycle influences the rate of reaction. This section is concerned with interpreting the observed reaction phenomena for NO + D₂ over Ir(110).

Although hysteresis in the rate of reduction of NO with H₂ over polycrystalline Pt was not reported [1], the distribution of the major products containing nitrogen (N₂ and NH₃) did vary in the same way as seen here for Ir(110). Under similar conditions, the maximum rate of production of ammonia is near 540 K on Ir(110) compared to 495 K on polycrystalline Pt [1]. The temperature at which 50% of the NO is reduced varies for Ir(110), but it is always higher than 445 K which was reported for polycrystalline Pt [1]. Also, the ratio of partial pressures (P_{D_2}/P_{NO}) required to achieve approximately the same fraction of NO converted to ND₃ is (qualitatively) higher for Ir(110) than Pt [1]. Thus, the postulate put forth in section 1 is verified, namely the activity of the Ir catalyst for the production of ammonia is lower than that of Pt, and this may be related to the observation that NO dissociates more readily on Ir than Pt. Although the steady state reaction was carried out over Pt(111) [2], the values of R used are much different from those employed here making comparisons of selectivity and activity with respect to Ir(110) difficult. Since the reduction reaction has not been studied on Rh under ultra-high vacuum conditions, it cannot be verified further that the activity of Ir is intermediate between Pt and Rh as suggested by the trend in the activity to dissociate NO.

Three regions of interest may be considered separately as suggested by the steady state reaction cycles. The first region is where N₂ is produced at a lower rate prior to the formation of a plateau (if there is one) and after the rate has passed through a second relative maximum above 500 K as the temperature increases. At this point, the conversion of the surface from one which is relatively free of oxygen

to one which is partially covered with oxide and chemisorbed oxygen and NO is complete. The second region is the plateau in the production of N₂ (and the production of D₂O by mass balance) which is insensitive to the surface temperature but is dependent upon the partial pressures of the reactants. The third region is the temperature and pressure regime under which the production of ammonia competes with the production of N₂ for nitrogen adatoms, i.e. for $R > 4$ and $470 < T < 630$ K, after the surface achieves a high rate of reduction of NO. In addition to these three regions, the transitions between the high and low rates of reduction of NO will be discussed.

6.1. Region 1. Low rate of N₂ production

As seen in figs. 5–7, the rate of production of N₂ is inhibited significantly in the region where the rate is not on a plateau as the temperature increases. The results in section 2 concerning the adsorption of deuterium on a saturated overlayer of coadsorbed NO and oxygen showed that deuterium is blocked almost completely from chemisorbing, whereas NO or oxygen alone did not block deuterium completely. In this region, the surface contains approximately a half ML of oxygen, at least a part of which is a surface oxide since the surface has reverted to the (1 × 1) unreconstructed structure from the (1 × 2) superstructure [21]. Also, the surface has a partial coverage of NO which varies with temperature due to a competition between desorption and adsorption of NO under steady state conditions. As the surface temperature increases, the rate of production of N₂ increases. However, N₂ cannot be produced unless the surface is reduced via the removal of oxygen by D₂. The empirical pressure dependence of the rate on the reactants, given by eq. (1) at a constant temperature, indicates that NO acts as a poison unlike D₂.

The dependence of the rate on P_{D_2} may be analyzed by considering the elementary steps involved in producing D₂O,



where S_{D_2} is the probability of adsorption of deuterium, and the various k_i are the rate coefficients of each elementary reaction. Applying the steady state approximation to adsorbed D and OD implies that

$$2S_{D_2}F_{D_2} - k_2\Theta_D^2 - 2k_3\Theta_O\Theta_D = 0, \quad (8)$$

where F_{D_2} is the impingement flux of D₂ (proportional to P_{D_2}) in the reactant beam. Under the conditions in this region, $2S_{D_2}F_{D_2}/k_2$ in eq. (8) is small compared

to $(k_3\Theta_O/k_2)^2$, and Θ_D is given approximately by

$$\Theta_D = S_{D_2}F_{D_2}/k_3\Theta_O. \quad (9)$$

Substituting eq. (9) into the expression for the rate of production of D₂O yields

$$R_{D_2O} = S_{D_2}F_{D_2}, \quad (10)$$

i.e. the proper dependence on P_{D_2} for the rate of production of N₂.

However, understanding the dependence of the rate on NO, $P_{NO}^{-1/2}$, is not so straightforward. It is appealing to think of NO as a poison since oxygen depleted by deuterium is supplied by the dissociation of NO. Moreover, NO will desorb, rather than dissociate if the coverage of oxygen is sufficiently large. The competition between the rate of removal of oxygen (R_{D_2O}), the rate of accumulation of oxygen via the dissociation of NO, and the rate of desorption of NO govern the rate of production of N₂.

Lastly, Arrhenius plots in fig. 9 give the effective activation energy for the steady state reaction, and it lies between 10.3 and 12.6 kcal mole⁻¹. It may be that this value represents the difference in activation energies for the desorption and the dissociation of NO. This would not be unreasonable since estimates of this difference in energy, in the absence of deuterium, place it near 8 kcal mole⁻¹ [17]. The rate limiting steps would be for NO to find an oxygen-free area in order to dissociate and for NO to desorb from areas containing adsorbed oxygen in order to allow deuterium to react away the oxygen. However, other elementary reactions are important, so that additional activation energy differences may be embodied in E .

6.2. Region 2. Plateau in N₂ production

For sufficiently high values of P_{D_2} compared to P_{NO} and sufficiently large temperatures, the low rate of production of N₂ in Region 1 becomes unstable, and a high rate occurs that does not depend sensitively on temperature over some range of temperature. In this second region, only conditions that produce the N₂ plateau and do not form ND₃ will be considered. As observed by both thermal desorption mass spectrometry and LEED, when the reaction is terminated during the steady state reaction on the N₂ plateau, the surface is a clean (1 × 2) substrate with small coverages of nitrogen and oxygen adatoms, unlike the surface conditions in Region 1. Although the oxygen adatoms present on the surface above 700 K are probably in an oxide form [21], they are in low concentration and still react readily with deuterium [27].

As seen in fig. 8 and quantified by the empirical expression in eq. (2), both NO and D₂ accelerate the rate in the plateau region. The linear dependence on P_{NO} in eq. (2) indicates that within the pressure range studied for NO, 5×10^{-8} to 4×10^{-7} Torr, the reaction to form N₂ (for a given P_{D_2}) is limited by the rate of dissociation of NO, so long as P_{D_2} is sufficiently large to maintain the plateau behavior. The dependence on P_{D_2} is easily understood in the plateau region by

examining the limit in eq. (8) for $2S_{D_2}F_{D_2}/k_2$ large compared to $(k_3\Theta_O/k_2)^2$ in order to obtain an approximate expression for Θ_D . Substituting this result into the expression for R_{D_2O} gives

$$R_{D_2O} = k_3 (2S_{D_2}F_{D_2}/k_2)^{1/2}\Theta_O, \quad (11)$$

where k_2 and k_3 appear in eqs. (5) and (6) for the desorption of D₂ and the reaction between deuterium and oxygen to form OD, respectively.

Over the pressure range of D₂ that is accessible (5×10^{-8} to 1×10^{-6} Torr), the rate of formation of N₂ depends on $P_{D_2}^{1/2}$. However, if larger pressures of D₂ were studied, the rate should reach a limiting value for a given P_{NO} . In this case, the rate should be limited by the flux of NO to the surface since the initial probability of adsorption is unity independent of temperature [17]. The $P_{D_2}^{1/2}$ dependence in Region 2 indicates that small coverages of oxygen influence the rate of dissociation compared to the rate of desorption of NO.

6.3. Region 3. Ammonia production

Ammonia is formed on Ir(110) between 470 and 630 K for values of R greater than four, depending also on the partial pressure of NO. It was found from XPS, UPS and LEED results that the surface is a (1×2) substrate with a partially ordered nitrogen $p(2 \times 2)$ superstructure near the ND₃ reaction maximum. Since ND_x ($x = 1, 2$) groups are not observed with either XPS or UPS if the reaction is terminated where ND₃ is produced, the rate limiting step to form ND₃ is $N + D \rightarrow ND$. The desorption of ND₃ is rapid in the reaction region in agreement with thermal desorption results for NH₃ on Ir(111), where NH₃ desorbs molecularly near 300 K [28].

Under conditions that produce ND₃ in competition with N₂, the empirical dependence of the rate of ND₃ production on the partial pressures of the reactants is given by $P_{D_2}^2 P_{NO}^{-1}$ (see eq. (4)). As in Region 1 where N₂ is produced at a low rate, NO acts as a poison by supplying oxygen that consumes deuterium which would otherwise react with nitrogen to form ND₃. A squared dependence on P_{D_2} may suggest that diffusion of deuterium adatoms in pairs is important, as was inferred near the rate maximum for CO oxidation on Ir(110) by the squared dependence on the pressure of oxygen [26]. Also, the stoichiometry of the reaction between NO and D₂ to form ND₃ and D₂O requires five deuterium adatoms for each NO ad molecule and would cause the rate to depend more strongly on P_{D_2} than on P_{NO} , although $N + D \rightarrow ND$ and $O + D \rightarrow OD$ are the rate limiting steps in the production of ND₃ and D₂O, respectively.

7. Summary

The reaction between NO and D₂ over Ir(110) has been studied under ultra-high vacuum conditions by means of measurements of the steady state rate of

reduction of NO as a function of the partial pressures of the reactants (5×10^{-8} to 1×10^{-6} Torr) and the surface temperature (300 to 1000 K). In addition, coadsorption studies of NO and deuterium at low temperature were performed to gain insight into the competitive nature of the chemisorption process and to observe the desorption characteristics of the coadsorbed overlayers as the surface is heated. The results of this investigation may be summarized as follows:

(1) Small precoverages of deuterium do not affect the kinetics of adsorption of NO but do affect the distribution of N₂ and NO that thermally desorbs from the surface. More N₂ desorbs when deuterium is present than in its absence due to the reaction between oxygen (from the dissociation of NO) and deuterium to form D₂O.

(2) The adsorption of deuterium is decreased, relative to the clean surface, when the latter is saturated with NO. However, D₂ is inhibited strongly from adsorbing when the surface is saturated with oxygen and NO, a condition that occurs under some steady state reaction conditions.

(3) Depending on the value of R , under steady state conditions a marked hysteresis can occur in the rate of reduction of NO. For certain values of R and the surface temperature, a plateau in the rate of reduction appears that persists as the temperature is decreased. At some temperature, depending upon P_{NO} and P_{D_2} , the rate falls precipitously to a new steady state where the rate of the reduction reaction is lower.

(4) For large values of R (>4), ND₃ is produced between 470 and 630 K and competes for nitrogen adatoms with the production of N₂.

(5) Three regimes of the steady state reaction were examined separately: (a) low rates producing only N₂ and D₂O with an inhibition by NO; (b) high rates with a plateau in the rate producing only N₂ and D₂O; and (c) high rates where N₂ and ND₃ are produced competitively. Explanations of the empirically observed rates were discussed in light of mass spectrometry, XPS, UPS, AES and LEED results.

References

- [1] G. Pirug and H.P. Bonzel, *J. Catalysis* 50 (1977) 64.
- [2] J.L. Gland, B.A. Sexton and E.B. Kollin, 7th Intern. Congr. on Catalysis, A3, Tokyo, 1980.
- [3] R.M. Lambert and C.M. Comrie, *Surface Sci.* 46 (1974) 61.
- [4] C.T. Campbell and J.M. White, *Appl. Surface Sci.* 1 (1978) 347.
- [5] T.P. Kobylinski and B.W. Taylor, *J. Catalysis* 33 (1974) 376.
- [6] K.C. Taylor and R.L. Klimisch, *J. Catalysis* 30 (1973) 478.
- [7] H. Conrad, G. Ertl, J. Küppers and E.E. Latta, *Faraday Disc. Chem. Soc.* 58 (1974) 116.
- [8] H. Conrad, G. Ertl, J. Küppers and E.E. Latta, *Surface Sci.* 65 (1977) 235.
- [9] H.P. Bonzel and G. Pirug, *Surface Sci.* 62 (1977) 45.
- [10] P.A. Thiel, W.H. Weinberg and J.T. Yates, Jr., *Chem. Phys. Letters* 67 (1979) 403.
- [11] G.E. Thomas and W.H. Weinberg, *Phys. Rev. Letters* 41 (1978) 1181.
- [12] E. Umbach, S. Kulkarni, P. Feulner and D. Menzel, *Surface Sci.* 88 (1979) 65.

- [13] J. Kanski and T.N. Rhodin, *Surface Sci.* 65 (1977) 63.
- [14] P.A. Zhdan, G.K. Boreskov, W.F. Egelhoff, Jr. and W.H. Weinberg, *J. Catalysis* 45 (1976) 281.
- [15] P.A. Zhdan, G.K. Boreskov, A.I. Boronin, A.P. Scheplin, W.F. Egelhoff, Jr. and W.H. Weinberg, *J. Catalysis* 60 (1979) 93.
- [16] J. Küppers and H. Michel, *Surface Sci.* 85 (1979) 201.
- [17] D.E. Ibbotson, T.S. Wittrig and W.H. Weinberg, *Surface Sci.* 110 (1981) 294.
- [18] D.E. Ibbotson, T.S. Wittrig and W.H. Weinberg, *J. Chem. Phys.* 72 (1980) 4885.
- [19] J.L. Taylor, D.E. Ibbotson and W.H. Weinberg, *J. Chem. Phys.* 69 (1978) 4298.
- [20] C.M. Chan, M.A. Van Hove, W.H. Weinberg and E.D. Williams, *Solid State Commun.* 30 (1979) 47; *Surface Sci.* 91 (1980) 400.
- [21] J.L. Taylor, D.E. Ibbotson and W.H. Weinberg, *Surface Sci.* 79 (1979) 349.
- [22] T.S. Wittrig, D.E. Ibbotson and W.H. Weinberg, *Surface Sci.* 102 (1981) 506.
- [23] G.B. Fisher and B.A. Sexton, *Phys. Rev. Letters*, submitted.
- [24] K. Kunimori, T. Kawai, T. Kondow, T. Onishi and K. Tamaru, *Surface Sci.* 59 (1976) 302.
- [25] G.G. Tibbetts and J.M. Burkstrand, *J. Vacuum Sci. Technol.* 15 (1978) 497.
- [26] J.L. Taylor, D.E. Ibbotson and W.H. Weinberg, *J. Catalysis* 62 (1980) 1.
- [27] D.E. Ibbotson, PhD Thesis, California Institute of Technology (1981).
- [28] R.J. Purtell, R.P. Merrill, C.W. Seabury and T.N. Rhodin, *Phys. Rev. Letters* 44 (1980) 1279.